PERFORMANCE OF STEGO IMAGES CALIBRATION USING ADVANCED DENOISING METHODS

Dmytro Progonov

***Abstract**: Reliable detection of messages that are unauthorized embedding into cover files, namely digital images, is topical task today. Design of effective stegdetectors is complicated by limited prior information of used adaptive embedding methods that minimize cover image alteration during data hiding. Modern approaches for improving detection accuracy are based on usage either ensembles of stegdetectors, or advanced neural networks, which characterize by high-computation complexity. This makes them inappropriate for real scenarios where fast re-tuning for detection of unknown embedding methods is needed. The alternative approach for stegdetector's design is based on modification of image pre-processing (calibration) methods, namely selection of methods for detection and extraction weak alteration of cover image features caused by message hiding. Special interest is taken to advanced methods for image denoising due to theirs high "adaptiveness" to statistical features of processed images that provide local processing of image's regions instead of global ones. The work is devoted to performance analysis of Total Variation Minimization (TVM) technique usage of calibration of stego images formed by adaptive embedding methods. According to obtained results we may conclude that applying of advanced TVM-based denoising methods does not allow considerably improving stegdetector detection accuracy in comparison with usage of standard SPAM model. On the other hand, applying of component analysis, namely Principal Component Analysis, allows considerably improve Matthews Correlation Coefficient (up to 0.3) for stegdetector in case of processing real images from MIRFlickr dataset. This can be explained by "grouping" of cover image alterations caused by message hiding into single component with the smallest energy (singular value) that makes possible its easy removal.*

***Keywords**: digital images steganalysis, adaptive embedding methods, component analysis methods.*

***ACM Classification Keywords**: Security and privacy – Systems security – Information flow controls*

***DOI**: https://doi.org/10.54521/ijita29-01-p01*

Introduction

Protection of critical information infrastructures of state agencies and enterprises is topical task today. Feature of these systems is integration with high-speed communications systems for remote operations and fast data sharing that complicates counteraction to sensitive information leakage during data transmission. The novel methods for concealed (steganographic) data transmission through publicly available channels allow considerably reducing efficiency of modern protection systems. This is achieved by usage of adaptive embedding methods that minimizes cover file, for example cover digital image, alterations by preserving fixed payload. Detection of formed stego images is non-trivial task due to limited prior information about used embedding methods that decrease accuracy of state-of-the-art statistical stegdetectors (SD).

Proposed approaches for improving accuracy of modern stegdetectors includes usage of ensembles of SD, cover image rich models, utilization of advanced neural networks architectures for revealing weak alterations of cover image's statistics caused by message hiding [Fridrich, 2009; Gribunin et al., 2018; Hassaballah, 2020]. Despite high detection accuracy of these stegdetectors, their practical usage is limited due to high computation complexity of tuning or re-training for detection of unknown embedding methods. For overcoming this limitation, there is proposed to improve image processing pipeline of SD instead of applying compute-intensive models [Progonov et al, 2020]. Usage of special design image pre-processing (calibration) methods for modern embedding methods allows considerably improving detection accuracy by preserving low-computation complexity of SD tuning procedure. Still, selection of effective calibration methods for processing of stego images formed by advanced adaptive embedding methods (AEM) remains unsolved task.

Feature of modern AEM is message embedding into highly textured (noised) regions of cover image by carefully selection of pixels set for preserving low level of CI alteration [Hassaballah, 2020]. Processing of these regions with widespread denoising methods, like Wiener filter or bilateral filters, does not allow detecting mentioned alterations due to "aggressive" processing of wide areas of image's pixels. On the other hand, information about performance analysis of advanced denoising methods for image calibration is limited in publicly available researches. These methods take of special interest in steganalysis due to adaptive processing of image by taking into account local statistical features.

The work is aimed at filling this gap by performance analysis of advanced denoising methods, namely Total Variation Minimization technique, for calibration of stego images formed by novel AEM. Obtained results allow making recommendation about usage of advanced image denoising methods in steganalysis related tasks.

Notations

High-dimensional arrays, matrices, and vectors will be typeset in boldface and their individual elements with the corresponding lower-case letters in italics. The symbols $\mathbf{U}=\left(u_{ij}\right)\in\Im^{N\times M}$, $\mathbf{X}=\left(x_{ij}\right)\in\Im^{N\times M}$ and $\mathbf{Y}=\left(y_{ij}\right)\in\Im^{N\times M}$, $\Im=\{0,1\ldots255\}$, will represent pixels brightness values of 8-bit grayscale initial (unprocessed), cover and stego images with size NxM pixels. The image's feature vector is denoted as $\mathbf{F}$, while the cover image payload (binary message) is represented as $\mathbf{M}$.

The Iverson bracket $\left[a\right]_I$ equals to one if the Boolean expression a is true, and zero otherwise. The notation $\|\cdot\|$ corresponds to Euclidean norm for scalar values, and Frobenius norm for matrices.

Related works

The accuracy of modern stegdetectors (SD) depends on many factors, including the availability of a priori data on the features of the steganographic method

used, statistical, spectral and structural parameters of the processed digital images (DI), methods of images pre-processing (calibration) etc. [Hassaballah, 2020]. Modern approaches to determining the factors that have the greatest impact on the quality of SD are based on the choice of a certain (fixed) structure of the stegdetector and further variation of individual parameters of SD to determine their impact on the accuracy of SD [Hassaballah, 2020; Gribunin et al., 2018]. This allows to quickly reconfiguring the SD by changing the parameters of only individual layers of neural networks, but determining the optimal values of these parameters by minimizing the error values of stego images classification P_E remains an unsolved problem for which heuristic methods are proposed for individual (partial) cases.

To overcome this limitation, the author proposes to combine individual parameters of the SD by the impact on detection accuracy, which simplifies the analysis of stegdetector performance and does not require the brute search of parameters values. This makes possible to present the value of the classification error P_E as a composition of the following functions that correspond to the main stages of image processing by stegdetector:

$$P_E = F_{calib}(\mathbf{I}) \circ F_{feature}(\tilde{\mathbf{I}}) \circ F_{class}(\mathbf{f}), \quad (1)$$

where $F_{calib}(\mathbf{I})$ – methods of image $\mathbf{I}$ pre-processing (calibration) that are aimed at detecting weak changes of cover image (CI) statistical parameters caused by message hiding; $F_{feature}(\cdot)$ – methods for determining the features of CI that change the most due to the message hiding; $F_{class}(\mathbf{f})$ – methods of image classification according to the results of the calculated vectors $\mathbf{f}$ (image parameters) processing.

The values of the functions $F_{feature}$ and F_{class} are the similar for the majority of stegdetectors, due to the common practice of using standard statistical models of CI, such as models SPAM [Pevny et al, 2010] and maxSRMd2 [Denemark et

al, 2014], as well as ensemble classifiers like Random Forest [Kodovsky et al, 2012]. This allows minimizing the value P_E while maintaining the low computational complexity of the stegdetector tuning. Therefore, research of advanced calibration methods for reliable detection and localization of CI distortions caused by message hiding pay special attention today.

In the paper [Kodovsky et al, 2009] it is proposed to present the influence of the image calibration methods on detection accuracy (1) as corresponding changes of positions of clusters of vectors related to statistical features of CI and formed stego images. These changes are schematically presented at Fig. 1.

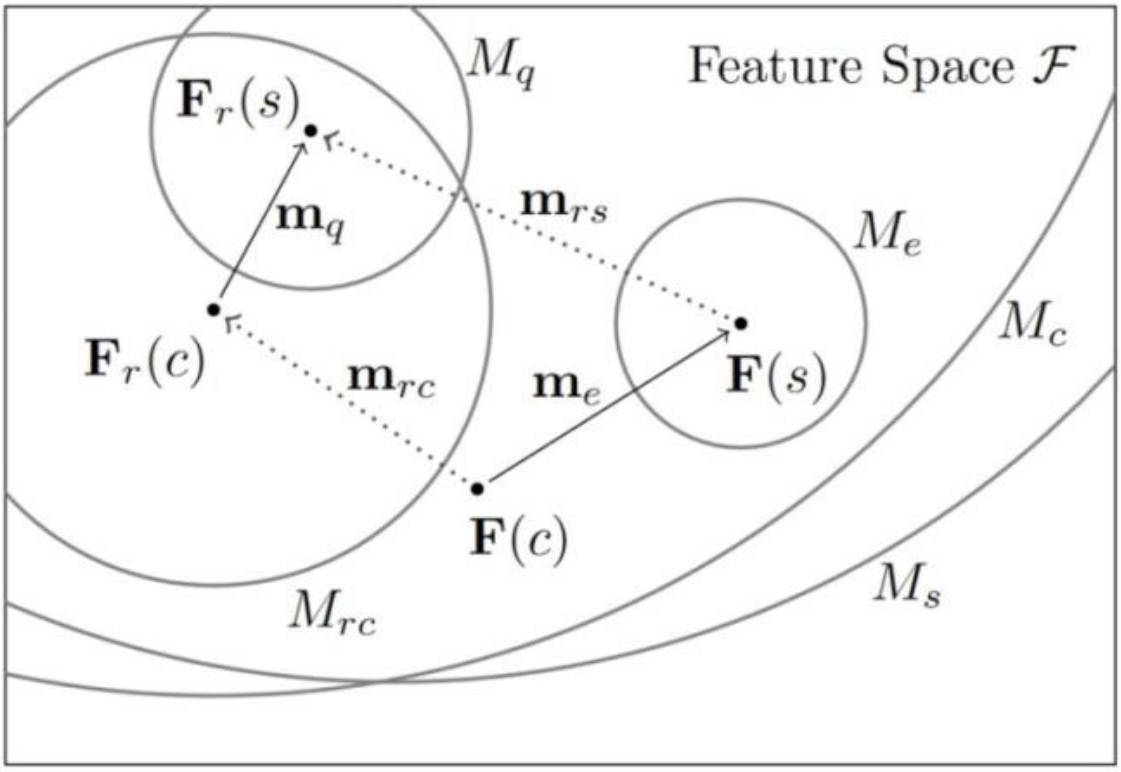

Figure 1 Schematic representation of the influence of image calibration methods on the mutual positions of clusters of vectors (statistical parameters) of cover and stego images. According to paper [Kodovsky et al, 2009].

Message embedding into a cover image leads to the shift of corresponding vectors $\mathbf{F}(c)$ to a new position $\mathbf{F}(s)$ that relates to statistical features of formed stego images. The magnitude of this shift can be estimated as the median $\mathbf{m}_e$ of the corresponding shifts for images from the test dataset. The sizes M_c and M_e of formed clusters $\mathbf{F}(c)$ та $\mathbf{F}(s)$ corresponds to the variability of statistical parameters for real cover images (Fig. 1).

Applying of image calibration methods F_{calib} to cover and stego images leads to the shift of clusters $\mathbf{F}(c)$ and $\mathbf{F}(s)$ to the corresponding values $\mathbf{m}_{rc}$ and $\mathbf{m}_{rs}$. As a result, the positions of the vectors of the processed images will correspond to the values $\mathbf{F}_r(c)$ and $\mathbf{F}_r(s)$, and the size of the new clusters will be equal to M_{rc} and M_q, respectively. Thus, minimization of detection error P_E in expression (1) requires selection of image calibration method F_{calib} that maximizes the value of the distance between clusters of cover and stego images clusters by preserving fixed size of these clusters.

Modern image calibration methods can be divided into the following groups depending on the impact on changes in the spatial position of clusters $\mathbf{F}_r(c)$ and $\mathbf{F}_r(s)$ [Kodovsky et al, 2009]:

- Parallel reference – these methods lead only to a parallel shift of the feature vectors cover and stego images, which does not increase the accuracy of the SD;
- Divergent reference (DR) – aimed at enhancing the differences between cover and stego images by increasing the distance between the respective feature vectors;
- Eraser – leads to significant decreasing of distance between feature vectors for cover and stego images, up to their full coincidence;
- Cover estimate (CE) – aimed at estimation of statistical characteristics of a cover image by analysis of available (noised) images. This leads to negligible changes of feature vectors for CI by providing considerable changes of features for stego image.

- Stego estimate (SE) – aimed at detection and amplification the distortions caused by message hiding into a CI. In this case, applying of these methods leads to insignificant alterations of stego images features, and drastically changes of CI features.

The schematic representation of clusters $\mathbf{F}(c)$ and $\mathbf{F}(s)$ mutual positions for considered cases is presented at Fig. 2.

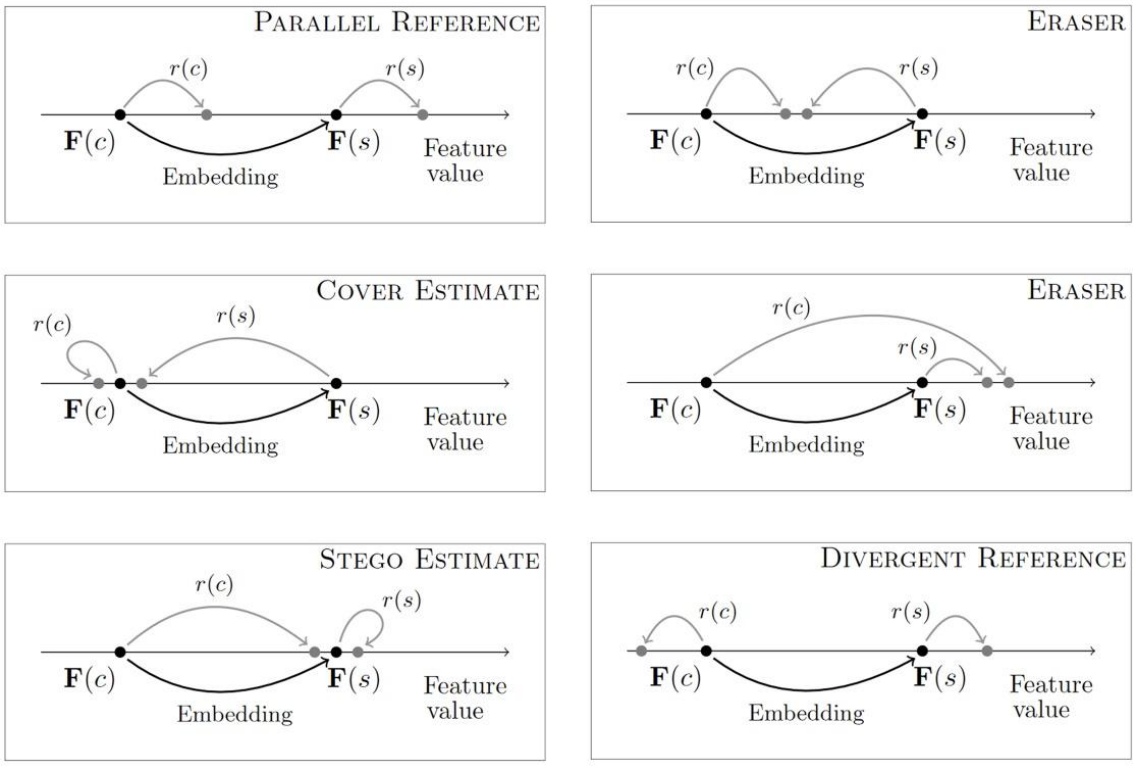

Figure 1 Schematic representation of the mutual positions of clusters of vectors (statistical parameters) of cover and stego images. According to paper [Kodovsky et al, 2009].

Modern researches of advanced calibration methods are aimed at finding effective DR-methods that maximize the distance between clusters of features vectors for cover and stego images in a given Euclidean space (Fig. 2). The position of these clusters can be estimated only approximately using available examples of cover and stego images due to limited capabilities of the

steganalytics to determine the features of used steganographic (embedding) method in the real cases. In the most difficult case of absence of a priori data about used embedding method, the steganalytics can estimate only position of feature vectors that correspond to the statistical parameters of cover images. This limits effectiveness of DR-like image calibration methods that requires information about mutual positions of both clusters $\mathbf{F}(c)$ and $\mathbf{F}(s)$ for estimation corresponding preimages from a higher dimensional space. Thus, optimal calibration method $\mathrm{K}_{opt}(\cdot)$ can be designed as method that estimates shift $d^{\mathbf{F}}_{\mathbf{X},\mathbf{Y}}$ of cover image's feature vector $\mathbf{f}(\mathbf{C})$ to a new positions $\mathbf{f}\left(\mathbf{Y},\Delta^S_\alpha\right)$ caused by stego images formation with a payload Δ^S_α :

$$\max_d d^{\mathbf{F}}_{\mathbf{X},\mathbf{Y}} = \max_{\mathbf{X},\mathbf{Y}} \left\| \mathbf{f}(\mathbf{X}) - \mathbf{f}\left(\mathbf{Y},\Delta^S_\alpha\right) \right\|_n, \tag{2}$$

where $\|\cdot\|_n$ – the function of estimating the distance between the feature vectors corresponding to the statistical parameters of cover $\mathbf{X}$ and stego $\mathbf{Y}$ images. As an example of such function, Euclidean metrics for multidimensional vectors can be used.

The maximum distance in expression (2) is reached in the case when vectors $\mathbf{f}(\mathbf{C})$ and $\mathbf{f}\left(\mathbf{Y},\Delta^S_\alpha\right)$ are located on opposite sides of the corresponding clusters $\mathbf{F}(c)$ and $\mathbf{F}(s)$. Therefore, the optimal transformation $\mathrm{K}_{opt}(\cdot)$ will correspond to the estimation of cover image's features from available (noisy) images (for CE-methods, K^{CE}_{opt}), or the removal of CI distortions caused by message embedding (for SE-methods, K^{SE}_{opt}):

$$\mathrm{K}^{CE}_{opt}(\mathbf{X},\mathbf{Y}) : \mathbf{Y}\left(\Delta^S_\alpha\right) \underset{\forall \Delta^S_\alpha \geq 0}{\rightarrow} \mathbf{X}, \tag{3}$$

$$\mathrm{K}^{CE}_{opt}(\mathbf{X},\mathbf{Y}) : \mathbf{X} \underset{\forall \Delta^S_\alpha \geq 0}{\rightarrow} \mathbf{Y}\left(\Delta^S_\alpha\right), \tag{4}$$

where the value $\Delta_{\alpha}^{S}=0\%$ corresponds to the case of cover image processing. Therefore, the stegdetector can be tuned using the following vectors (statistical parameters of the analyzed images) after applying of transformations (3)-(4) [Progonov et al, 2020; Progonov, 2021]:

$$\mathbf{F}_{LF}=a\cdot F_{cal}^{M}\left(\mathbf{U}\right)+b\cdot F^{M}\left(\mathbf{U}\right), \tag{5}$$

$$\mathbf{F}_{CC}=\left\{F^{M}\left(\mathbf{U}\right);F_{cal}^{M}\left(\mathbf{U}\right)\right\},$$

where $a,b\in \mathrm{R}-$ are weights; $F^{M}\left(\cdot\right),F_{cal}^{M}\left(\cdot\right)-$ vectors that correspond to the statistical parameters of the initial and calibrated images, estimated with a statistical model M respectively; $\mathbf{F}_{LF}-$ vectors corresponding to the linear form of the vectors of initial and processed DI; $\mathbf{F}_{CC}-$ relates to the union (Cartesian calibration) of features for initial and processed images.

In the general case, the values of the coefficients a and b in expression (5) can be chosen arbitrarily, but for practical applications the following cases take special interest:

$$\mathbf{F}_{nc}=\mathbf{F}_{LF}\big|_{a=0,b=(+1)}=F^{M}\left(\mathbf{U}\right),$$

$$\mathbf{F}_{calib}=\mathbf{F}_{LF}\big|_{a=(+1),b=0}=F_{cal}^{M}\left(\mathbf{U}\right), \tag{6}$$

$$\mathbf{F}_{DF}=\mathbf{F}_{LF}\big|_{a=(+1),b=(-1)}=F_{cal}^{M}\left(\mathbf{U}\right)-F^{M}\left(\mathbf{U}\right), \tag{7}$$

where vectors $\mathbf{F}_{nc}$ and $\mathbf{F}_{calib}$ correspond to the statistical parameters of the initial and processed images $\mathbf{U}$, while $\mathbf{F}_{DF}-$ represents the difference of these vectors.

Based on the results of using transformations K_{opt}^{CE} (3) and K_{opt}^{SE} (4), it becomes possible to calculate vectors $\mathbf{F}_{calib}$ (6) and $\mathbf{F}_{DF}$ (7). Note, that values of these vectors will be the same while considered transformations (3)-(4) are aimed at

determining the statistical parameters of cover image (CE-based calibration) or detect its distortions due to a message embedding (SE-based calibration). This makes vectors (6)-(7) ineffective for SD tuning. On the other hand, the length of the vectors $\|\mathbf{F}_{DF}\|_2$ (7) will be proportional to the magnitude of the cover image's features change caused by message hiding. Also, the value of the vectors $\mathbf{F}_{DF}$ length will be non-zero only for stego images (for CE-based calibration), which simplifies the detection of these images by using simple threshold methods for obtained feature vectors. Similarly, the value $\|\mathbf{F}_{DF}\|_2$ will be nonzero for CI when using SE-based calibration, as a result of which we can conclude about the duality of transformations (3)-(4).This leads to the fact that applying of these transformations for SD tuning will lead to the same accuracy of stego images detection, which will be determined only by the features of used cover model and type of classifier. Therefore, further studies will provide results only for the use of the transformation K_{opt}^{CE}.

Task and challenges

The paper is devoted to performance analysis of applying component analysis methods, namely principal component analysis (PCA), and advanced image denoising techniques, such as TVM-methods, for calibration of stego images formed according to novel adaptive embedding methods MG and MiPOD.

Digital images steganalysis based on image pre-processing methods

The modern approach to the design of the transformation K_{opt}^{CE} (3) is usage of spectral methods of image processing in order to reduce the impact of distortions caused by messages hiding [Fridrich, 2009]. These methods are based on the assumption that the statistical parameters of interference in digital images are known [Mallat, 2008]. In particular, the assumption that the noise is evenly distributed over frequency bands is used in most cases, which allows to effectively suppressing their impact by thresholding coefficients of two-dimensional discrete wavelet transform (2D-DWT). However, alterations caused by message embedding can be distributed only certain areas of the image and do not have an ordered structure due to applying of advanced adaptive

embedding methods. Distribution of 2D-DWT coefficients related to these alterations among several frequency sub-bands leads to decreasing of mentioned thresholding methods.

To overcome this limitation, it is of interest to use advanced denoising methods that allows adaptively tune pixels values depending on theirs variance. One of such methods is Total Variation Minimization (TVM) filtering based on decreasing of variance of image pixel brightness values: [Mallat, 2008; Rudin et al., 1992]:

$$\mathrm{V}(\mathbf{U}) = \sum_{x,y} \sqrt{\left|\mathbf{U}_{x+1,y} - \mathbf{U}_{x,y}\right|^2 + \left|\mathbf{U}_{x,y+1} - \mathbf{U}_{x,y}\right|^2}, \quad (8)$$

where $\mathbf{U}$ is analyzed grayscale image with size of $N \times M$ pixels.

Then, the task of estimation of initial (not noised) cover image from current (noised) image can be presented as a optimization problem of minimization the overall level of variation in the brightness of the pixels of the image:

$$\min_{\mathbf{U}} \left(\|\mathbf{U}\|_2^2 + \lambda \cdot \mathrm{V}(\mathbf{U}) \right), \quad (9)$$

where $\|\mathbf{U}\|_2^2 -$ image energy estimation; $\lambda > 0 -$ regularization weight of variation $\mathrm{V}(\mathbf{U})$ influence on image energy. Note that estimation (8) is not a differentiated function that limits usage of known optimization methods to solve the problem (9). Therefore, in most cases, an approximate estimation is used [Chambolle, 2004]:

$$\mathrm{V}_{anis}(\mathbf{U}) = \sum_{x,y} \left|\mathbf{U}_{x+1,y} - \mathbf{U}_{x,y}\right| + \left|\mathbf{U}_{x,y+1} - \mathbf{U}_{x,y}\right|.$$

A variety of methods for solving the optimization problem (11) by usage of approximation $\mathrm{V}_{anis}(\mathbf{U})$, such as Bregman [Getreuer, 2012] and Chambolle [Chambolle, 2004] methods. The feature of these methods is the representation

of the initial optimization problem in the following equivalent form [Getreuer, 2012]:

$$\min_{\mathbf{U}\in \mathrm{BV}(\Omega)} \|\mathbf{U}\|_{\mathrm{TV}(\Omega)} + \frac{\lambda}{2}\int_{\Omega}\left(\tilde{\mathbf{U}}-\mathbf{U}\right)^2 dxdy, \qquad (10)$$

where $\mathrm{BV}(\Omega)-$ set of functions with limited variation of values in the region Ω; $\mathrm{TV}(\Omega)-$ the operator for estimation signal's values variance in the region Ω; $\lambda > 0-$ weight parameter of regularization; $\tilde{\mathbf{U}}-$ estimation of the un-noised image after application of the TVM method. In the case of processing smooth signals, in particular images, the operator $\mathrm{TV}(\Omega)$ is equivalent to calculating the signal gradient ∇:

$$\|\mathbf{U}\|_{\mathrm{TV}(\Omega)} = \int_{\Omega}\|\nabla\mathbf{U}\|_2\, dxdy.$$

Then the optimization problem (10) can be solved using the Euler-Lagrange method by solving the following nonlinear elliptic equation in partial derivatives [Getreuer, 2012]:

$$\begin{cases} \nabla\cdot\left(\dfrac{\nabla_{\mathbf{U}}}{\|\nabla\mathbf{U}\|_2}\right)+\lambda\cdot\left(\tilde{\mathbf{U}}-\mathbf{U}\right)=0, & \mathbf{U}\in\Omega, \\ \dfrac{\partial\mathbf{U}}{\partial x\partial y}=0, & \mathbf{U}\in\partial\Omega. \end{cases}$$

A limitation of practical usage of TVM-methods for image calibration is high computational complexity that can be important factor for intrusion detection systems.

The alternative approach to design the transformation K_{opt}^{CE} is usage of component analysis methods based on signal decomposition into components by the criterion of theirs statistical characteristics. One of the well-known methods of component analysis is PCA. This method is based on the signal

decomposition into orthogonal components by the criterion of maximization the energy of these components [Comon et al., 2010; Cichocki et al., 2002]:

$$\sum_{i=1}^{m} \left\| \mathbf{x}_i - L_k \right\|_2^2 \to \min, \tag{11}$$

where $\mathbf{x}_i \in \mathrm{R}^N, i \in [1;m]$ – i$^{\text{th}}$ element of the set of vectors; $L_k \subset \mathrm{R}^N$ – manifold for used set of vectors. The approximation (11) can be represented by k-dimensional linear manifold in the space R^N – a set of linear combinations $L_k = \left\{ \mathbf{a}_0 + \beta_1 \mathbf{a}_1 + \cdots + \beta_k \mathbf{a}_k \middle| \beta_i \in \mathrm{R}, i \in [1;k] \right\}$, where $\{\mathbf{a}_0, \cdots, \mathbf{a}_k\} \subset \mathrm{R}^N$ – the orthonormal set of vectors. Then expression (16) can be represented in the following form [Comon et al., 2010]:

$$\left\| \mathbf{x}_i - L_k \right\|_2^2 = \left\| \mathbf{x}_i - \mathbf{a}_0 - \sum_{j=1}^{k} \mathbf{a}_j \cdot \left\langle \mathbf{a}_j, \mathbf{x}_i - \mathbf{a}_0 \right\rangle \right\|_2^2, \tag{12}$$

The solution of the optimization problem (12) for $k \in [0;n)$ can be represented by a set of nested spaces $L_0 \subset L_1 \subset \cdots \subset L_{n-1}$. These spaces are determined by the orthonormal set of vectors (vectors of principal components) $\{\mathbf{a}_1, \cdots, \mathbf{a}_{n-1}\}$ and the vector $\mathbf{a}_0$. Each of the vectors $\mathbf{a}_i$ can be found as a solution of the minimization problem for L_i using the generalized least squares method [Comon et al., 2010]:

$$\mathbf{a}_i = \arg\min_{\mathbf{a}_i \in \mathrm{R}^N} \left(\sum_{j=1}^{m} \left\| \mathbf{x}_j - L_i \right\|_2^2 \right), \tag{13}$$

Therefore, the problem of finding the main components (13) can be reduced to the equivalent problem of diagonalization of the covariance matrix $\mathbf{C}$:

$$c_{ij} = \frac{1}{m-1} \sum_{l=1}^{m} \left(x_{li} - \bar{\mathbf{X}}_i \right) \cdot \left(x_{lj} - \bar{\mathbf{X}}_j \right),$$

where $\mathbf{X} = \{\mathbf{x}_1, \ldots, \mathbf{x}_m\}^{\mathrm{T}}, \mathbf{x}_i \in \mathrm{R}^N -$ the matrix formed from the row-vectors; $\bar{\mathbf{X}}_k$ – the mean value of the k[th] row of matrix $\mathbf{X}$.

Then, PCA corresponds to the spectral decomposition of the covariance matrix $\mathbf{C}$ – the representation of the data space in the form of the sum of mutually orthogonal eigenspaces C_i. The matrix $\mathbf{C}$ can be represented as a linear combination of orthogonal projection operators on these spaces with weights $\lambda_i \geq 0, \forall i$. Therefore, the problem of spectral decomposition of the matrix $\mathbf{C} = \mathbf{X}^{\mathrm{T}}\mathbf{X}/(m-1)$ is equivalent to the problem of singular decomposition of the data matrix $\mathbf{X}$ by PCA [Comon et al., 2010].

The principal component analysis is widely used for noise reduction in signals, such as digital images, since it does not require a priori data on the statistical features of the image. The noise corresponds to the components of the image with the smallest singular numbers. This allows usage of threshold methods for processing singular numbers to suppress noise, even under limited a priori data on their statistical characteristics. Mentioned features of PCA make it the attractive candidate for image calibration task in DI steganalysis.

Adaptive embedding methods

The state-of-the-art embedding methods for digital images are based on minimizing the empirical function $D(\mathbf{X}, \mathbf{Y})$ used for estimation distortion a cover image $\mathbf{X}$ during forming a stego image $\mathbf{Y}$ [Filler et al, 2011]:

$$D(\mathbf{X}, \mathbf{Y}) = \sum_i \rho_i(\mathbf{X}, \mathbf{Y}) \to \min, |\mathbf{M}| = const, \tag{14}$$

where $\rho_i(\cdot)$ – function for estimation alteration of cover's statistical characteristics caused by embedding of i[th] stegobit; $|\mathbf{M}|$ – size of embedded message $\mathbf{M}$ in bits. Minimization of function (14) allows adapting the embedding process to used cover image $\mathbf{X}$, thus corresponding steganographic methods called adaptive.

In most cases, the choice of function $D(\mathbf{X},\mathbf{Y})$ is performed using assumption of distortions additivity, namely independency of distortions caused by embedding of individual stegobits. This simplifies choice of function (14) by the cost of reducing accuracy of tracking interactions between distortions that may lead to non-linear changes of CI parameters.

During research, we considered the case of usage the novel adaptive embedding methods MG [Sedighi et al, 2015] and MiPOD [Sedighi et al, 2016]. These methods are aimed at message $\mathbf{M}$ embedding into spatial domain by manipulation with brightness of individual pixels of a cover. Let us consider these methods in details.

The advanced approach to design an empirical function $D(\mathbf{X},\mathbf{Y})$ in eq. (14) is based on minimization cover image distortions as well as detectability of formed stego images [Ker et al, 2013]. This approach is used in considered MG and MiPOD embedding methods by applying of locally-estimated multivariate Gaussian model for estimate statistical features of CI. This makes possible achieving stego image's security close to advanced steganographic methods by preserving relatively low computation complexity.

Formation of stego images according to Mg and MiPOD methods is carried out in several steps [Sedighi et al, 2016]. At first, the context of cover image $\mathbf{X}=(x_1,\ldots,x_{M\cdot N})$ is suppressed by using denoising filter F:

$$\mathbf{r}=\mathbf{X}-F(\mathbf{X}),$$

where $\mathbf{X}$ is represented in column-wise order. Then, the variance σ_l^2 of residual $\mathbf{r}$ pixels brightness is estimated by applying of Maximum Likelihood Estimation (MLE) method:

$$\mathbf{r}_l=\mathbf{G}\mathbf{a}_l+\xi_l,$$

where $\mathbf{r}_l$ – represents the value of the residuals $\mathbf{r}$ inside the $p\times p$ block surrounding of l[th] pixel of residual; $\mathbf{G}_{p^2\times p}$ – the matrix defines parameters of MLE model; $\mathbf{a}_{p\times 1}$ – the

vector of model's parameters mean values; $\boldsymbol{\xi}_{p^2\times 1}$ – the signal whose variance is need to be estimated.

At the second step, the variance σ_l^2 is estimated according to the following formula:

$$\sigma_l^2 = \left\| \mathbf{P}_{\mathbf{G}}^{\perp} \mathbf{r}_l \right\|^2 \Big/ \left(p^2 - q \right),$$

where $\mathbf{P}_{\mathbf{G}}^{\perp} = \mathbf{I}_l - \mathbf{G}\left(\mathbf{G}^T\mathbf{G}\right)^{-1}\mathbf{G}^T$ – the orthogonal projection of residual $\mathbf{r}_l$ to the $p^2 - q$ dimensional subspace spanned by the left eigenvectors of matrix $\mathbf{G}$; $\mathbf{I}_{l\times l}$ – the unity matrix.

The feature of MG embedding method [Sedighi et al, 2015] is usage of simplified variance estimator in comparison with MiPOD method:

$$\sigma_l^2 = \left\| \mathbf{r}_n - \hat{\mathbf{r}}_n \right\|^2 \Big/ \left(p^2 - q \right),$$

$$\hat{\mathbf{r}}_n = \mathbf{G}\left(\mathbf{G}^T\mathbf{G}\right)^{-1}\mathbf{G}^T\mathbf{r}_n.$$

Thirdly, the probability of l[th] embedding change $\beta_l, l \in \{1,2,\ldots,L\}$ that minimize the deflection coefficient ς^2 between cover and stego image distributions is determined:

$$\zeta^2 = 2\sum_{l=1}^{M\cdot N} \beta_l^2 \sigma_l^{-4}, \tag{15}$$

under constrain

$$R = \sum_{l=1}^{M\cdot N} H\left(\beta_l\right),$$

where $H(z) = -2z\log z - (1-2z)\log(1-2z)$ – ternary entropy function; R – cover image payload in nats.

Minimization of (15) can be achieved by using the method of Lagrange multipliers. The change rate β_l and the Lagrange multiplier λ can be determined by solving of following $(l+1)$ equations:

$$\beta_l \sigma_l^{-4} = \frac{1}{2\lambda} \ln\left(\frac{1-2\beta_l}{\beta_l}\right), l \in [1; M \cdot N],$$

$$R = \sum_{l=1}^{M \cdot N} H(\beta_l).$$

Then, the estimated change rate β_l is converted to the corresponding cost ρ_l of CI features alterations by stego bit embedding into l^{th} pixel of cover image:

$$\rho_l = \ln(1/\beta_l - 2). \quad (16)$$

Finally, the message $\mathbf{M}$ is embedded using syndrome-trellis codes (STCs) with costs determined according to formula (16).

Usage the locally-estimated multivariate Gaussian model for estimate statistical features of CI for considered MG and MiPOD methods allows to capture the non-stationary character of natural images as well as derive a closed-form expression for estimation statistical detectability of formed stego images [Sedighi et al, 2016].

Experiments

Performance analysis of cover image estimation methods was done for stego images formed according to state-of-the-art adaptive MG and MiPOD embedding methods was considered. The cover image payload was changed from 3% to 5% with step 2%, from 5% to 10% with step 5%and from 10% to 50% with step 10%.

Evaluation was performed on standard ALASKA and MIRFlickr datasets:

- The ALASKA dataset [Cogranne et al, 2019] is one of standard datasets for performance evaluation of modern stegdetectors. The dataset includes 80,000 images captured by 40 cameras, including smartphones, tablets, low-end cameras to high-end full frame digital single-lens reflex camera. The images were converted from raw files by variation of demosaicing algorithm, resizing, image compression methods etc.

- The MIRFlickr dataset [Huiskes et al, 2008] is part of open evaluation project of real image forensics and retrieval. The dataset consists of digital images gathered from the Flickr service coupled with manual annotations, pre-computed descriptors and EXIF data. The images from the datasets are characterized by high variability of pre-processing history (such as resizing, re-compression, visual enhancement). This makes MIRFlickr dataset the attractive candidate for performance evaluation of SD in the environment as close as possible to the real cases of natural images processing.

During research, the sub-sets of 10,000 DI were sampled from each of mentioned datasets. The images were converted to grayscale format (if they were colored) with usage of standard function "rgb2gray" from MATLAB computing platform. Finally, images were cropped to preserve similar size of 512x512 pixels.

The image calibration was performed with usage of PCA and TVM methods. The percentage of PCA components that were remained during image processing was varied in the following range – 90%, 95%, 97% and 99%. The image denoising with usage of TVM methods was performed according to Chambolle [Chambolle, 2004] and Bregman [Getreuer, 2012] methods. The application of these transformations leads to a change of the statistical characteristics of processed images. According to the results [Progonov et al, 2020; Progonov, 2021], usage of vectors $\mathbf{F}_{DF}$ (9) as feature vectors to stegdetector tuning allows significantly reducing the error P_E in comparison with usage of statistical features of processed images.

The statistical SD based on standard SPAM [Pevny et al, 2010] cover model was used for estimation baseline detection accuracy. The SPAM model is based on applying of first and second order Markov chain for adjacent pixels brightness correlation modeling. Evaluation of trained SD was done using standard cross-validation procedure by 10-times splitting of used datasets into train (70%) and test (30%) subsets. The SD was trained for minimization of the classification error P_E [Kodovsky et al, 2012]:

$$P_E = \min_{P_{FA}} \frac{1}{2}\left(P_{FA} + P_{MD}\left(P_{FA}\right)\right),$$

where P_{FA} and P_{MD} are probability of false alarm and missed detection, respectively.

Also, it is investigated the influence of a prior information about used embedding method on SD performance. This is modeled by variation the fraction of pairs cover and corresponding stego images in the training set S_{train}. The following indicator was used to quantify this proportion during stegdetector tuning [Progonov, 2020]:

$$K_{\alpha}^{OL} = \left|\left\{\left(\mathbf{X},\mathbf{Y}\right):\left(\mathbf{X}_i,\mathbf{Y}_i\right), i \in S_{train}\right\}\right| \Big/ \left|S_{train}\right| \times 100\%.$$

The value of K_{α}^{OL} indicator varies from 0%, which corresponds to the case of absence in set S_{train} cover images for presented stego images, to 100% when train set includes only pairs cover and corresponding stego images. During the research, we considered the case of $K_{\alpha}^{OL} = 0\%$ that corresponds to a situation when steganalytics does not have access to the stego encoder and can use only the available stego images (zero-day problem).

Matthews Correlation Coefficient MCC was used to assess the performance of tuned SDs. The coefficient is used to estimate the degree of correlation of the (true) labels of the classes of the studied images with output of stegdetector [Chicco et al., 2020]:

$$MCC = \frac{P_{TP} \times P_{TN} - P_{FP} \times P_{FN}}{\sqrt{\left(P_{TP} + P_{FP}\right) \cdot \left(P_{TP} + P_{FN}\right) \cdot \left(P_{TN} + P_{FP}\right) \cdot \left(P_{TN} + P_{FN}\right)}},$$

where P_{TP} – the probability of correct classification of stego images; P_{TN} – the probability of correct classification of CI; P_{FP} – the probability of incorrect

classification of cover images as stego ones; P_{FN} – the probability of incorrect classification of stego images as cover ones.

The value of the Matthews Correlation Coefficient varies from (-1) that corresponds to the case of incorrect classification of stego images as cover ones and vice versa, to (+1) that relates to correct classification of both cover and stego images. A special case is the value $MCC = 0$ that corresponds to the case of assigning the analyzed image to the classes of cover or stego images randomly ($P_{FP} = P_{FN}$).

Research of image calibration with usage of TVM and PCA methods was done in several stages. Firstly, the performance of TVM methods applying to cover and stego images was considered. The dependencies of Matthews Correlation Coefficient *MCC* on cover image payload for MG (a) and MiPOD (b) embedding methods by the usage of Total Variation Minimization methods for image calibration on ALASKA dataset is presented at Fig. 3.

Usage of standard SPAM model allows considerably (ΔMCC=0.12) improving MCC values in comparison with advanced maxSRMd2 model in the case of low cover image payload (less than 10%, Fig. 3). Increasing of cover image payload leads to corresponding improving detection accuracy for maxSRMd2 model that overcome SD based on SPAM model for high payload range (more than 20%). Note, applying of TVM-methods for digital images calibration does not improve MCC values in comparison with SPAM model for both considered MG (Fig. 2a) and MiPOD (Fig. 3b) embedding methods. This can be explained by high quality of test images from ALASKA dataset [Cogranne et al, 2019] (low level of image's intrinsic noises) that complicates message hiding. Therefore, applying of TVM methods leads to removing both intrinsic noises, and alterations caused by message hiding.

For comparison, it is represented dependencies of Matthews Correlation Coefficient *MCC* on cover image payload for MG (a) and MiPOD (b) embedding methods by the usage of Total Variation Minimization methods for image calibration on MIRflickr dataset at Fig. 4.

a)

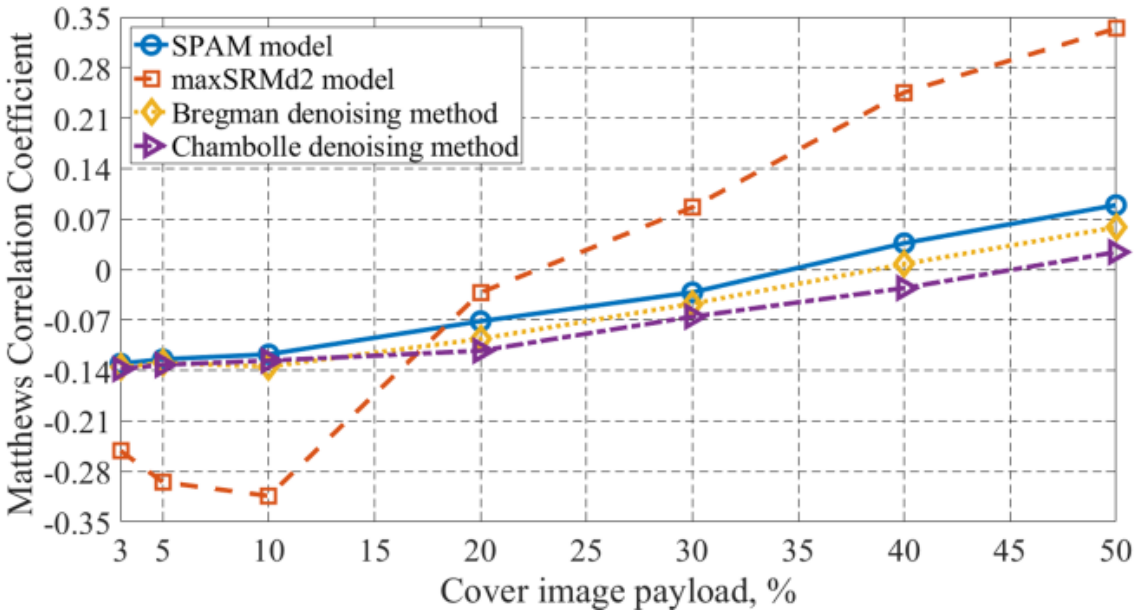

b)

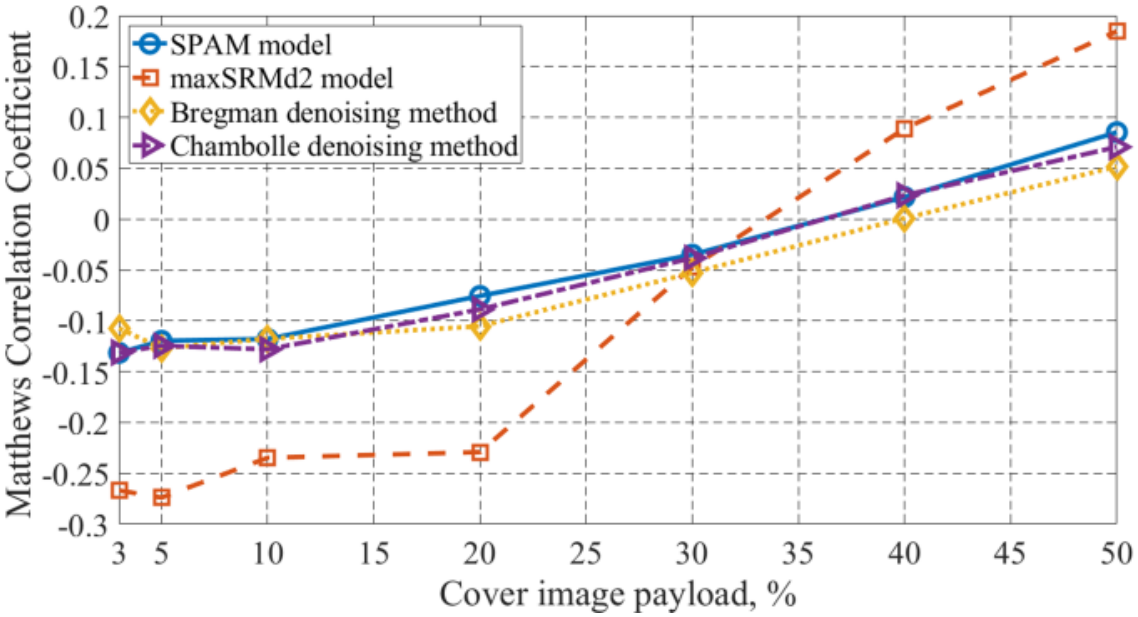

Figure 3. The dependencies of Matthews Correlation Coefficient *MCC* on cover image payload for MG (a) and MiPOD (b) embedding methods by the usage of Total Variation Minimization methods for image calibration on ALASKA dataset.

a)

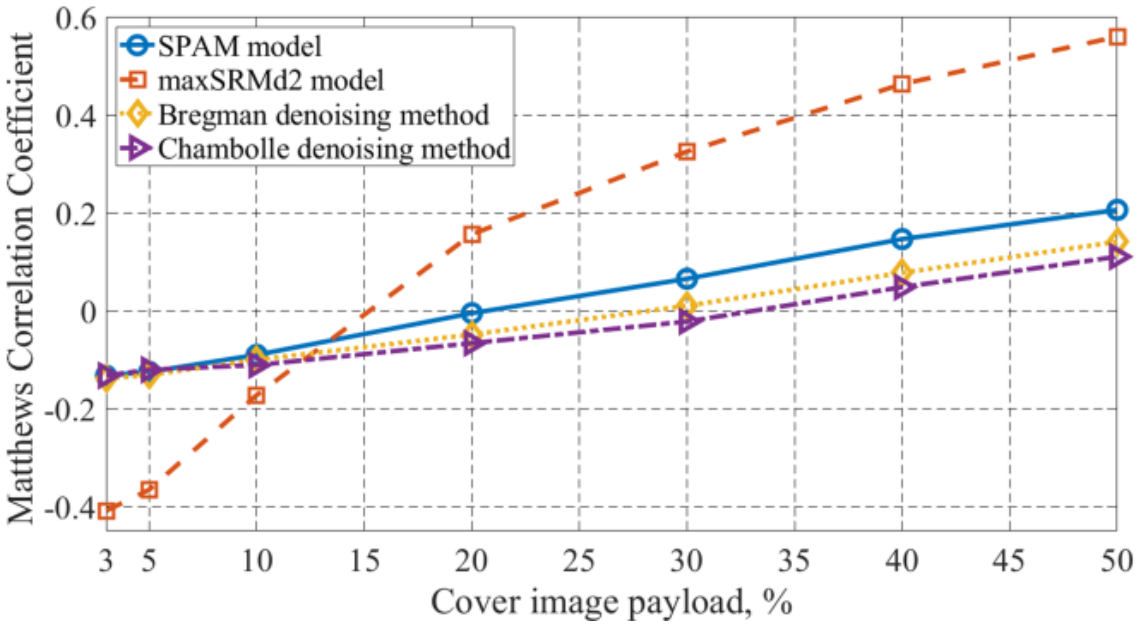

b)

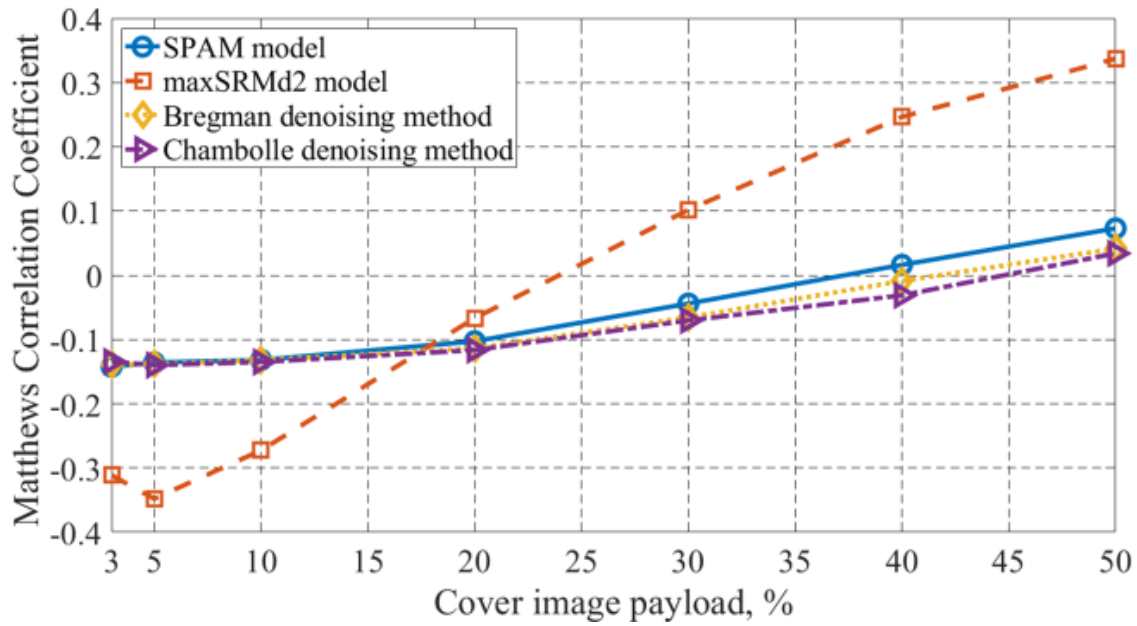

Figure 4. The dependencies of Matthews Correlation Coefficient *MCC* on cover image payload for MG (a) and MiPOD (b) embedding methods by the usage of Total Variation Minimization methods for image calibration on MIRFlickr dataset.

Real images from MIRFlickr dataset [Huiskes et al, 2008] characterize relatively high level of intrinsic noises that simplifies message embedding by considered MG and MiPOD methods. Nevertheless, usage of ensemble of high-pass filters for maxSRMd2 model (Fig.4) allows accurately extract these noises for further analysis. The estimated values of Matthews Correlation Coefficient *MCC* by applying of TVM-based calibration methods for stego images formed by MG and MiPOD embedding methods for test images sampled from ALASKA and MIRFlickr datasets and low (5%) and high (50%) cover image payload are presented at Tab. 1.

Table 1. The estimated values of Matthews Correlation Coefficient *MCC* by applying of TVM-methods calibration methods for stego images formed by MG and MiPOD embedding methods for test images sampled from ALASKA and MIRFlickr datasets and low (5%) and high (50%) cover image payload

Image calibration method	MG embedding method		MiPOD embedding method	
	ALASKA dataset	MIRFlickr dataset	ALASKA dataset	MIRFlickr dataset
Low cover image payload (5%)				
No calibration (SPAM model)	-0.1245	-0.1249	-0.1197	-0.1358
No calibration (maxSRMd2 model)	-0.2949	-0.3654	-0.2739	-0.3479
Bregman denoising method	-0.1296	-0.1314	-0.1172	-0.1384

Image calibration method	MG embedding method		MiPOD embedding method	
	ALASKA dataset	MIRFlickr dataset	ALASKA dataset	MIRFlickr dataset
Chambolle denoising method	-0.1322	-0.1205	-0.1246	-0.1399
High cover image payload (50%)				
No calibration (SPAM model)	0.0894	0.2058	0.0854	0.0730
No calibration (maxSRMd2 model)	0.3343	0.5595	0.1847	0.3372
Bregman denoising method	0.0586	0.1407	0.0759	0.0415
Chambolle denoising method	0.0242	0.1103	0.0709	0.0340

Applying of considered TVM-methods for image calibration leads to improving of MCC values of in stegdetector in comparison with standard SPAM model even for middle cover image payload (more than 10%, Tab. 1). On the other hand, usage of considered TVM methods does not allow to improve detection accuracy of SD even by analysis of real (noised) images in comparison with previous case (Fig. 3) – difference between estimated MCC values for image calibration with TVM method and SPAM model is about 0.1.

Therefore, we may conclude that applying of advanced TVM methods for image denoising does not allow considerably improving detection accuracy in comparison with case of applying the standard SPAM model of cover image. Obtained results can be explained by high "adaptability" of message embedding into cover image's intrinsic noises by usage of MG and MiPOD method. This decrease efficiency of image calibration with TVM methods while these methods are aimed at minimization of total variation of pixel brightness, so suppression of weak changes of pixels brightness is negligible. Thus, it represents the interest to apply PCA method for image decomposition and further usage of components with smaller energy (singular values) for detection of these changes. The dependencies of Matthews Correlation Coefficient *MCC* on cover image payload for MG (a) and MiPOD (b) embedding methods by the usage of Principal Component Analysis for image calibration on ALASKA dataset is presented at Fig. 5.

Applying of PCA allows negligibly improving of MCC values (up to 0.02) for MG embedding method (Fig. 5a), by preserving up to 97% energy of analyzed image. On the other hand, detection accuracy for SD based on image calibration with PCA is even decreased in comparison with case of usage the standard SPAM model (Fig. 5b). This can be explained by message embedding in noise components of image by MG method that can be detected and removed with PCA, while MiPOD embedding method spread these alterations among several components. For comparison, it is represented dependencies of Matthews Correlation Coefficient *MCC* on cover image payload for MG (a) and MiPOD (b) embedding methods by the usage of Principal Component Analysis methods for image calibration on MIRflickr dataset at Fig. 6.

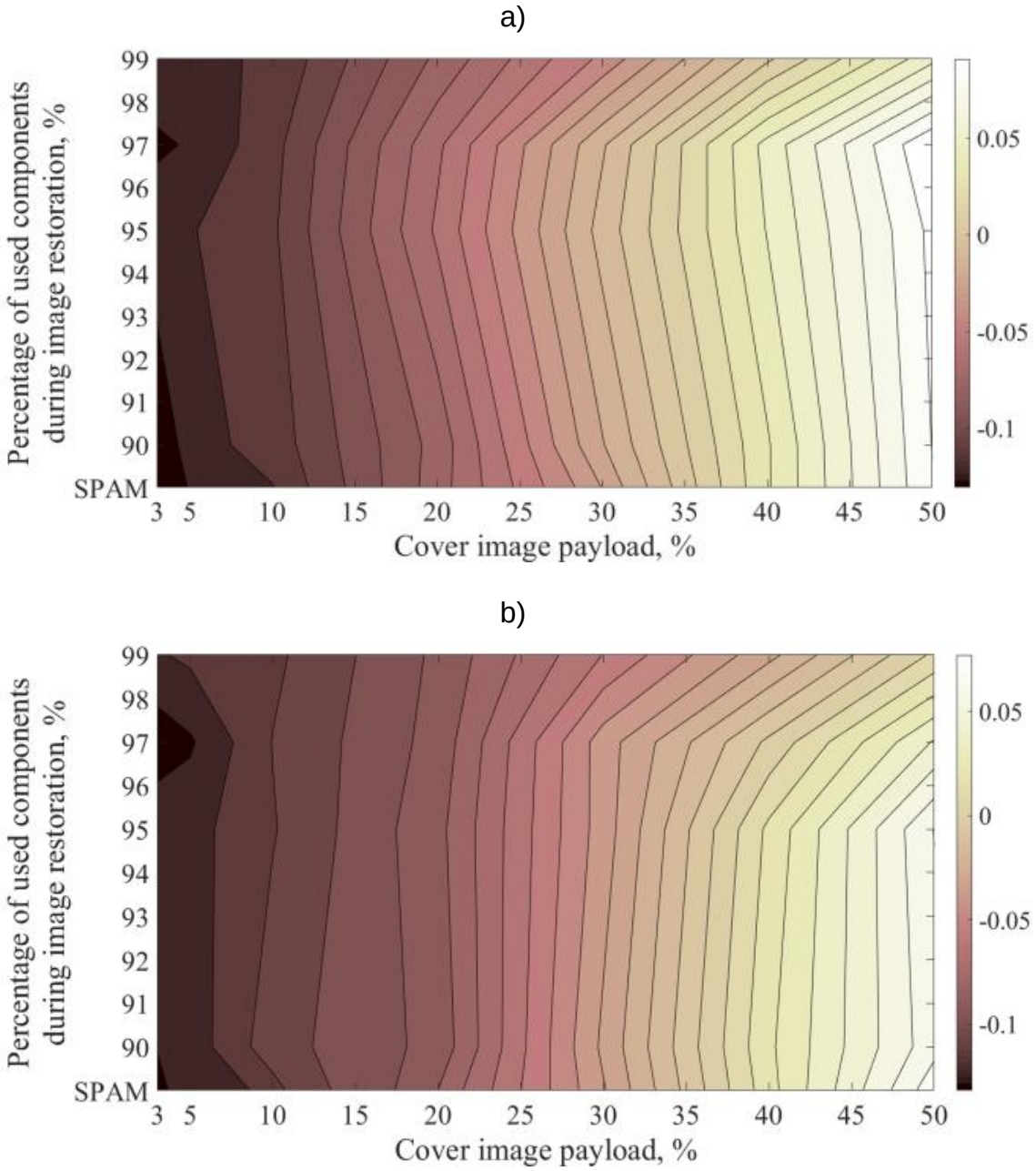

Figure 5. The dependencies of Matthews Correlation Coefficient *MCC* on cover image payload for MG (a) and MiPOD (b) embedding methods by the usage of Principal Component Analysis for image calibration on ALASKA dataset. The "*SPAM*" label denotes the case of SPAM model usage.

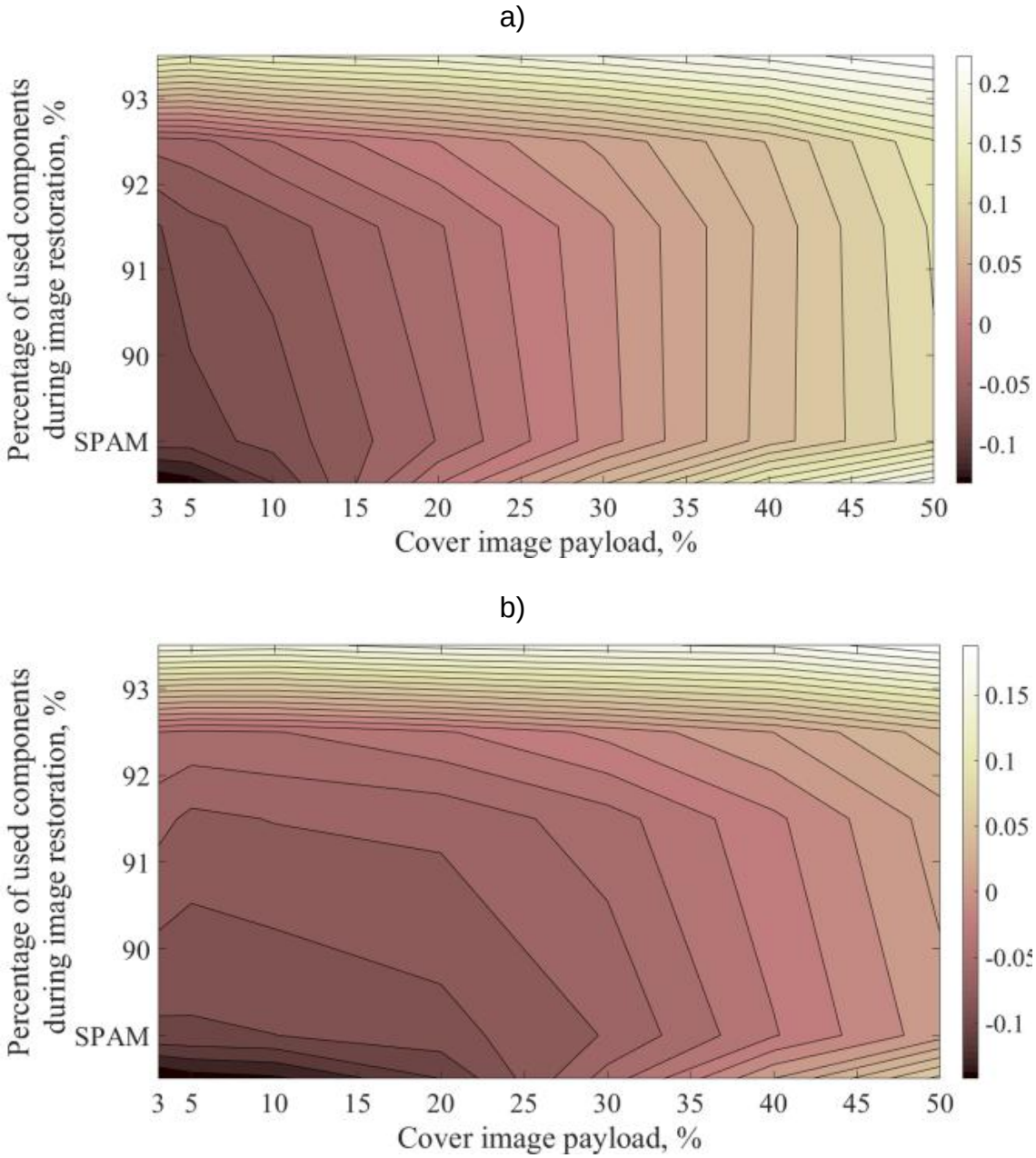

Figure 6. The dependencies of Matthews Correlation Coefficient *MCC* on cover image payload for MG (a) and MiPOD (b) embedding methods by the usage of Principal Component Analysis for image calibration on MIRFlickr dataset. The "*SPAM*" label denotes the case of SPAM model usage.

Applying of PCA for real images from MIRFlickr dataset (Fig. 6) leads to considerable improving of MCC values (up to 0.3) by removing the components with the smallest singular vales. The estimated values of Matthews Correlation Coefficient *MCC* by applying of PCA calibration methods for stego images formed by MG and MiPOD embedding methods for test images sampled from ALASKA and MIRFlickr datasets and low (5%) and high (50%) cover image payload are presented at Tab. 2.

Table 2. The estimated values of Matthews Correlation Coefficient *MCC* by applying of PCA calibration methods for stego images formed by MG and MiPOD embedding methods for test images sampled from ALASKA and MIRFlickr datasets and low (5%) and high (50%) cover image payload

Image calibration method	MG embedding method		MiPOD embedding method	
	ALASKA dataset	MIRFlickr dataset	ALASKA dataset	MIRFlickr dataset
Low cover image payload (5%)				
No calibration (SPAM model)	-0.1245	-0.1249	-0.1197	-0.1358
No calibration (maxSRMd2 model)	-0.2949	-0.3654	-0.2739	-0.3479
PCA (90% thresholding)	-0.1168	-0.0826	-0.1197	-0.0919
PCA (95% thresholding)	-0.1136	-0.0660	-0.1181	-0.0664

Image calibration method	MG embedding method		MiPOD embedding method	
	ALASKA dataset	MIRFlickr dataset	ALASKA dataset	MIRFlickr dataset
High cover image payload (50%)				
No calibration (SPAM model)	0.0894	0.2058	0.0854	0.0730
No calibration (maxSRMd2 model)	0.3343	0.5595	0.1847	0.3372
PCA (90% thresholding)	0.0913	0.1200	0.0656	0.0105
PCA (95% thresholding)	0.0934	0.1257	0.0690	0.0223

Revealed effect of *MCC* values improving by applying of PCA for image calibration preserves even for small cover image payload (less than 10%) for both considered embedding methods (Tab. 2). Therefore, we may conclude that PCA is promising candidate for calibration of real images that characterizes high level of intrinsic noises.

Conclusion

In the paper we investigated performance of advanced denoising methods as well as component analysis methods for image calibration during stegdetector tuning. The case of detection a stego images formed according to advanced MG and MiPOD adaptive embedding methods was considered.

According to obtained results we may conclude that applying of advanced Total Variation Minimization denoising methods does not allow improving stegdetector detection accuracy in comparison with usage of standard SPAM model. This can be explained by low "adaptiveness" of this method – image denoising is achieved by reducing total variation of pixels brightness irrespectively to variation of individual pixels. On the other hand, applying of component analysis, namely Principal Component Analysis, allows considerably (up to 0.3) improve MCC values for stegdetector in case of processing real images from MIRFlickr dataset. This can be explained by "grouping" of cover image alterations caused by message hiding into single component with the smallest energy (singular value) that makes possible its easy removal. Therefore, we may conclude that component analysis methods are promising candidates for further development of advanced image calibration methods that preserves high detection accuracy even for advanced adaptive embedding methods.

Bibliography

[Chambolle, 2004] Chambolle, A. An algorithm for total variation minimization and applications. Journal of Mathematical Imaging and Vision. 20, pp. 89–97, 2004, DOI:10.1023/B:JMIV.0000011325.36760.1e.

[Chicco et al., 2020] Chicco D., Jurman G. The advantages of the Matthews correlation coefficient (MCC) over F1 score and accuracy in binary classification evaluation. BMC Genomics, vol. 21, 2020. DOI: 10.1186/s12864-019-6413-7.

[Cichocki et al., 2002] Cichocki A., Amari S. Adaptive Blind Signal and Image Processing, 1st edition. Wiley, 586 p., 2002. ISBN: 978-0471607915.

[Cogranne et al, 2019] Cogranne R., Giboulot Q., Bas P. The ALASKA Steganalysis Challenge: A First Step Towards Steganalysis. ACM Workshop on Information Hiding and Multimedia Security, pp. 125-137, 2019. DOI: 10.1145/3335203.3335726.

[Comon et al., 2010] Comon P., Jutten C. Handbook of Blind Source Separation: Independent Component Analysis and Applications, 1st edition. Academic Press, 856 p., 2010. ISBN: 978-0123747266.

[Denemark et al, 2014] Denemark T., Sedighi V., Holub V., Cogranne R., Fridrich J. Selection-Channel-Aware Rich Model for Steganalysis of Digital Images. IEEE Workshop on Information Forensic and Security, Atlanta, GA, 2014. DOI: 10.1109/WIFS.2014.7084302

[Filler et al, 2011] Filler T., Fridrich J. Design of Adaptive Steganographic Schemes for Digital Images. Proc. SPIE, Electronic Imaging, Media Watermarking, Security, and Forensics XIII, 2011, DOI: 10.1117/12.872192.

[Fridrich, 2009] J. Fridrich Steganography in Digital Media: Principles, Algorithms, and Applications. 1st edition. Cambridge University Press, 2009. p. 437. ISBN 978–0–521–19019–0;

[Getreuer, 2012] Getreuer P. Rudin–Osher–Fatemi Total Variation Denoising using Split Bregman. Image Processing On Line, 2, pp. 74-95, 2012. DOI:10.5201/ipol.2012.g-tvd.

[Gribunin et al., 2018] Gribunin V., Okov I., Turintsev I. Digital steganography, 2nd edition, Moskow, SOLON-Press, 2018, ISBN: 978-5-91359-173-9 (In Russian).

[Hassaballah, 2020] M. Hassaballah, Digital Media Steganography: Principles, Algorithms, and Advances, 1st edition, New York: Academic Press, 2020, ISBN: 9780128194386.

[Huiskes et al, 2008] Huiskes M. J., Lew M.S. The MIR Flickr Retrieval Evaluation. ACM International Conference on Multimedia Information Retrieval, Canada, 2008. DOI: 10.1145/1460096.1460104

[Ker et al, 2013] Ker A. D., Bas P., Böhme R., Cogranne R., Craver S., Filler T., Fridrich J., Pevný T. Moving steganography and steganalysis from the laboratory into the real world. Proceedings of the first ACM workshop on Information hiding and multimedia security (IH&MMSec '13). New York, 2013. DOI: 10.1145/2482513.2482965

[Kodovsky et al, 2009] J. Kodovsky, J. Fridrich. Calibration revisited. Multimedia and Security Workshop, Princeton, 2009, DOI: 10.1145/1597817.1597830.

[Kodovsky et al, 2012] Kodovsky J., Fridrich J., Holub V. Ensemble Classifiers for Steganalysis of Digital Media. IEEE Trans. Inf. Forensics Security, vol. 7, issue 2, 2012, pp. 432-444. DOI: 10.1109/TIFS.2011.2175919

[Mallat, 2008] Mallat S. A Wavelet Tour of Signal Processing: The Sparse Way, 3rd edition. Academic Press, 2008. 832 p., ISBN: 978-0123743701.

[Pevny et al, 2010] Pevny T., Bas P., Fridrich J. Steganalysis by Subtractive Pixel Adjacency Matrix. IEEE Trans. Inf. Forensics Security, vol. 5, issue 2, 2010, pp. 215-224. DOI: 10.1109/TIFS.2010.2045842

[Progonov, 2020] Progonov D. Performance of Statistical Stegdetectors in Case of Small Number of Stego Images in Training Set. IEEE International Scientific-Practical Conference "Problems of Infocommunications Science and Technology" (PIC S&T 2020). 2020. DOI:10.1109/PICST51311.2020.9467901.

[Progonov et al, 2020] Progonov D., Lucenko V. Steganalysis of adaptive embedding methods by message re-embedding into stego images. Information Theories and Applications. Vol. 27, Issue 4. 2020. pp. 3-24.

[Progonov, 2021] Progonov D.O. Detection Of Stego Images With Adaptively Embedded Data By Component Analysis Methods. Advances in Cyber-Physical Systems (ACPS), Vol. 6, Number 2, 2021, pp. 146-154.

[Rudin et al. 1992] Rudin, L. I.; Osher, S.; Fatemi, E. Nonlinear total variation based noise removal algorithms. Physica D. 60 (1–4), pp. 259–268, 1992, DOI:10.1016/0167-2789(92)90242-f.

[Sedighi et al, 2015] Sedighi V., Fridrich J., Cogranne R. Content-Adaptive Pentary Steganography Using the Multivariate Generalized Gaussian Cover Model. Proc. SPIE, Electronic Imaging, Media Watermarking, Security, and Forensics, 2015, vol. 9409. DOI: 10.1117/12.2080272

[Sedighi et al, 2016] Sedighi V., Cogranne R., Fridrich J. Content-Adaptive Steganography by Minimizing Statistical Detectability. IEEE Trans. Inf. Forensics Security. Vol. 11, Iss. 2., 2016. pp. 221-234. DOI: 10.1109/TIFS.2015.2486744

Authors' Information

Dmytro Progonov *– Institute of Physics and Technology, National Technical University of Ukraine "Igor Sikorsky Kyiv Polytechnic Institute"; PhD, Associate Professor; 37, ave. Peremohy, Solomenskiy district, Kyiv, Postcode 03056, Ukraine; e-mail: progonov@gmail.com*

Major Fields of Scientific Research: digital media steganalysis, digital image forensics, machine learning, advanced signal processing